Influence of Volatile Fatty Acid Concentration on Biogas Production in Synthropic Anaerobic Digestion

by Nazaruddin Sinaga

Submission date: 10-Jan-2020 02:02PM (UTC+0700)
Submission ID: 1240580030
File name: 2.pdf (2.44M)
Word count: 4788
Character count: 24237

Penerbit Akademia Baru

Journal of Advanced Research in Biofuel and Bioenergy

Journal homepage: www.akademiabaru.com/arbb.html
ISSN: 2600-8459

Influence of Volatile Fatty Acid Concentration on Biogas Production in Synthropic Anaerobic Digestion

Open Access

Nazaruddin Sinaga[1,*], Maizirwan Mel[2], Rezeki Pakpahan[1], Nor Azwadi Che Sidik[3]

ARTICLE INFO

Article history:
Received 5 November 2017
Received in revised form 15 December 2017
Accepted 21 December 2017
Available online 31 December 2017

ABSTRACT

Keywords:
Volatile Fatty Acid, anerobic digestion, biogas, synthropic, numerical method, CFD

1. Introduction

Nowadays, the availability of energy from fossil fuels is not proportional to the amount of energy consumption at any time. Growing industry as well as population growth led to an increase

* *Corresponding author.*
E-mail address: nsinaga.ccfed@yahoo.com (Nazaruddin Sinaga)

in energy demand. Therefore, new energy sources are needed to meet the energy needs, especially those generated from industrial waste or other waste. One potential source used as a renewable energy source is biogas, which can be formed through the process of anaerobic digestion in a reactor. The main factors of biogas production are 4 components, namely: substrates, microorganisms, environmental conditions, and operating reactors or technology used [1]. Because now in many countries have been applied various technologies to produce biogas which can then be used as electrical energy.

Biogas is produced from the anaerobic digestion process, in which the organic compound of the substrate will be degraded by microbiological activity in a state without oxygen. Anaerobic digestion is divided into 4 stages, namely hydrolysis, acidogenesis, acetogenesis, and metanogenesis [2, 3]. To produce optimum biogas, a mixer is needed in digester, which serves as a mixer between the substrate and water to do reaction to produce optimal biogas and keep the temperature balance on the digester [4]. The mixer also plays a role in accelerating the out rate of biogas that has been generated to immediately leave the digester for unsaturated digester chamber so that anaerobic digging process can run optimally. Because of its role, the mixer on the digester is a very vital component in producing optimal biogas.

Biogas formation is a complex series of biochemical processes and involves several types of anaerobic microorganisms. In an anaerobic digester, synthropic reactions are considered to be the process steps that limit the formation of this biogas. To study and understand the processes occurring within this stirred digester, one of the prospective methods used is to use a numerical or Computational Fluid Dynamic (CFD) method. This method can simulate mass transfer, momentum, and energy aspects, in steady or transient conditions, in 3-dimensional basis, with single or multiphase, both in reacting and unreacted mixtures, in both laminar and turbulent flow regimes [5]. Research on numerical simulations using CFDs has been done by many researchers [6-8], but simulated anaerobic digestions using three phases with substrate variations have not been done by anyone.

In this study, the raw material used in the simulation is volatile fatty acid (VFA), which is the result of degradation in acidogenesis process. These results are propionic acid, butyric and acetate [9]. The three acids are then reacted in this simulation resulting in biogas in the digester. In anaerobic digestion process, volatile fatty acids are produced at the acidogenesis stage through the breakdown of proteins, carbohydrates and fats. Volatile fatty acids produced in the form of acetic acid, propionic acid, and butyric acid. Acetic acid can be directly degraded to methane, whereas propionic acid and butyrate cannot be directly degraded to methane so that it is first degraded into acetic acid and then degraded again to methane. This is because the methanogen bacteria group can only act with acetic acid. The process that has dependence between groups of methanogens and acetogenic bacteria is called syntrophic interaction [10]. The degradation of these three types of acids follows the equation of the reactions given in Table 1 below. This reaction is used as the basis for simulation in this study.

Table 1
Equation of reactions

Compound	Reaction
Propionic acid degradation	$CH_3CH_2COOH + 2H_2O \rightarrow CH_3COOH + CO2 + 3H_2$
Butyric acid degradation	$CH_3CH_2CH_2COOH + 2H_2O \rightarrow 2CH_3COOH + 2H_2$
Acetic acid	$CH_3COOH \rightarrow CO_2 + H_{2+}CH_4$

2. Methodology

2.1 Experimental Data

This research uses experimental data of Amani et al [11] as a simulation reference. In the experiment, an anaerobic digestion process was conducted in a stirred digester with the raw material of a synthetic chemical compound of volatile fatty acids (VFA). Then, the VFA is mixed with the acetogenic and methanogenic bacterial groups obtained from the degradation process of the material from the milk waste in another UASB (Upflow Anaerobic Sludge Bed) type digester. Then obtained data result of digestate form of biogas which consists of some compound such as methane, carbon dioxide and hydrogen. This experiment result data is used as a reference to validate the simulation run. In Table 2 shows the experimental results used as validation data.

Table 2
Experimental data for results validation [11]

Time		Concentration (mg/L)
(hour)	(second)	
0	0	1500
11.5	41,400	1,159.6
21.0	75,600	643.6
30.5	109,800	630.8

2.2 The Eulerian Multiphase Model

The multi-level Eulerian model is the most complex multiphase model found in the ANSYS FLUENT Software by solving the momentum and continuity equations for each phase used. The breakdown of this momentum and continuity equation depends on the type of phase mixture used, whether granular flow (fluid-solid) or non-granular flow (fluid-fluid). For granular flow, flow properties can be obtained based on kinetic theory. The multicular Eulerian model allows multiphasic modelling to be separated, but interactable. Phases may involve fluid, gas, or solids. The equations of multicular Eulerian builders are solved sequentially, the non-linear equations are then linearised to produce the dependent variable equations in each calculation. The resulting linear system is then broken down to produce a flow-field solution. An implicit point (Gauss-Seidel) linear as an equation solver is used in the relationship of multi-grid methods to solve scalar systems resulting from equations for the dependent variables in each cell [12]. In the Eulerian multiphasic model the continuity equation for phase-i is determined by the equation

$$\frac{\partial}{\partial t}(\alpha_i p_i) + \nabla . (\alpha_i p_i \vec{v}_i) = 0 \quad (1)$$

where $\vec{v}_i$ is the velocity of phase-i.
For the momentum conservation equation each phase-i is:

$$\frac{\partial}{\partial t}(\alpha_i p_i \vec{v}_i) + \nabla . (\alpha_i p_i \vec{v}_i \vec{v}_i) = -\alpha_i \nabla . \bar{\bar{\tau}}_i + \alpha_i p_i g + \sum_{i=1}^{n} \vec{R}_{ji} + \alpha_i p_i (\overrightarrow{F_i}) \quad (2)$$

where $\bar{\bar{\tau}}_i$ is stress-strain tensor of phase-i, which can be calculated from equation:

$$\bar{\bar{\tau}}_i = \alpha_i \mu_i \left(\nabla \vec{v}_i + \vec{v}_i^{\,T}\right) + \alpha_i \left(\lambda_i - \frac{2}{3}\mu_i\right) \nabla . \vec{v}_i \bar{I} \quad (3)$$

with μ_i and λ_i is the shear and bulk viscosity of the i-phase [13].

2.3 Turbulence Model

The turbulence model used in this research is the k-ε RNG model. This model is derived using meticulous statistical methods (group renormalization theory). This model is an improvement of the standard k-epsilon method, so the form of equation used is similar. Improvements contained in this RNG model include: the RNG model has an additional magnitude of the dissipation rate equation (epsilon), thus increasing accuracy for a suddenly blocked flow. Swirling effects on turbulence have also been provided, thus increasing the accuracy for swirl flow types. It has also provides an analytical formulation for turbulent Prandtl numbers, while the standard k-epsilon model uses a constant user-defined Prandtl number. The RNG model provides formulations for low Reynold numbers, while the standard k-epsilon model is a model for the high Reynolds number. In the RNG model *k-ε* kinetic energy and energy dissipation is calculated using the equation:

$$\frac{\partial}{\partial t}(\rho_m \varepsilon) + \nabla \cdot (\rho_m \overrightarrow{v_m} \varepsilon) = \nabla \cdot \left(\frac{\mu_{t,m}}{\sigma_\varepsilon} \nabla \varepsilon\right) + C_{1\varepsilon} G_{k,m} - C_{2\varepsilon} \rho_m \varepsilon \quad (4)$$

$$\frac{\partial}{\partial t}(\rho_m k) + \nabla \cdot (\rho_m \overrightarrow{v_m} k) = \nabla \cdot \left(\frac{\mu_{t,m}}{\sigma_\varepsilon} \nabla k\right) + G_{k,m} - \rho_m \varepsilon \quad (5)$$

The turbulent viscosity of the *i*-phase is calculated by the equation

$$\mu_{t,m} = \rho_m C_\mu \frac{k^2}{\varepsilon} \quad (6)$$

The parameters of the mixed properties are calculated by the equation

$$\rho_m = \sum_{i=1}^{n} \alpha_i p_i \quad (7)$$

The standard values of RNG parameters used in the setting are: $c_{m\mu}$ = 0.0845, $c_{1\text{-epsilon}}$ = 1.42, $c_{2\text{-epsilon}}$ = 1.68, dispersion Prandtl number = 1.0, dispersion Reynold number = 1.3.

2.4 Species Transport Equation

The species transport equation is a conservation equation for determining the equality of chemical species within the CFD. When this equation is enabled, the CFD will calculate and predict the local mass fraction in each species (Yi) by using the convection-diffusion equation in each species-i. The general form of the species transport equation is

$$\frac{\partial}{\partial t}(pYi) + \nabla . (pvYi) = -\nabla . Ji + Ri \quad (8)$$

where *Ji* is the flux diffusion from species-i and Ri is the quantity of production of species-i based on biochemical reactions. For turbulent flow, diffusion flux is obtained from the equation

$$Ji = \left(pD_{i,m}\frac{\mu_t}{Sc_t}\right)\nabla \text{Yi} \quad (9)$$

where $D_{i,m}$ is the diffusion coefficient of species i and Sct is the Schmidt turbulent number.

2.5 Population Balance Equation

Population balance equation is a model equation that regulates bubble phenomena in multiphase flow. Through this equation CFDs can predict bubble growth rates, ranging from emerging to the loss of bubbles in the multiphase flow. This phenomenon is governed by two process rules, namely the process of breakage and aggregation process. Breakage set in the process of bubble appearance, while aggregation set the process of bubble loss. The general equation of the population balance equation is

$$\frac{\partial}{\partial t}[n(V,t)] + \nabla.[un(V,t)] = B_{ag} - D_{ag} + B_{br} - D_{br} \quad (10)$$

where, D_{ag}, B_{ag}, D_{br}, B_{br} describe the rate of bubble occurrence on volume V, based on the aggregation process, and the rate of bubbles loss in volume V, based on the breakage process [14].

2.6 Geometry Design

Continuous stirred bioreactor is one type of vertical tubular reactor with a mixer in the middle. In modelling, the geometry of the continuous stirred bioreactor is done by two stages, starting from making component of stirred bioreactor, then put together in assembly. Figure 1 shows the geometry of the digester and mixer [15], whereas in Table 3 the dimensions of the main parameters of digester and mixer are shown.

Table 3
Dimensions of the digester and mixer

Parameter	Dimension (mm)
Inlet, Outlet Diameter	8
Length of Column	120
Digester Height	165
Diameter of Column	6
Digester Diameter	120
Blade Thickness	2
Blade Length	8
Blade Width	10
Impeller Disk Diameter	30
Impeller Disk Thickness	2

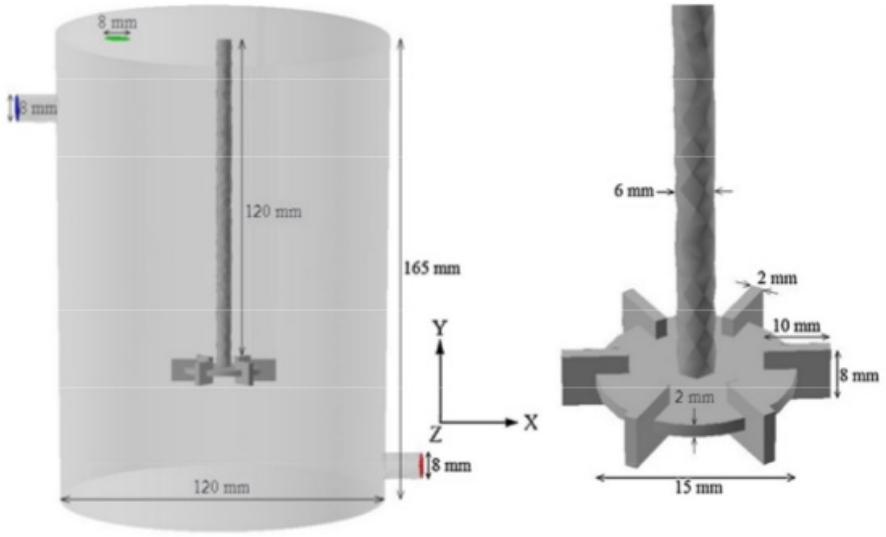

Fig. 1. Geometry of CSTR digester

2.7 Boundary Conditions

The model boundary conditions used in this simulation are shown in Fig. 2 and Table 4.

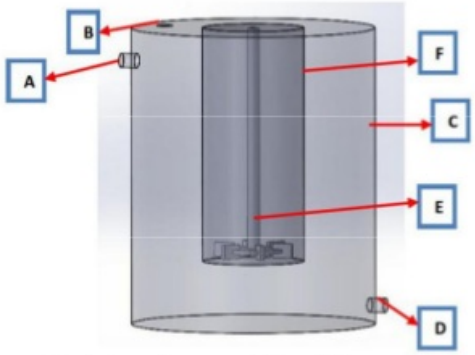

Fig. 2. Boundary condition of the model

Table 4
Boundary conditions of the model

Boundary condition	Surface	Bondary Condition
A	Inlet	Velocity Inlet
B	Biogas Outlet	Pressure Outlet
C	Digester Wall	Wall
D	Sludge Outlet	Pressure Outlet
E	Impeller	Wall
F	MRF	Interface

2.8 Meshing

The mesh size applied to the model affects the accuracy of CFD analysis. The smaller the mesh size on the model, the more accurate the results obtained, but require longer computing power and time compared to mesh that has a larger size. ANSYS Fluent can solve many cases with different types and forms of mesh (grid). There are many types of grids, namely grid O, grid C, triangular grid, tetrahedral grid, square grid and hexahedral grid. In this simulation mesh is used according to the desired grid of the tetrahedral grid with 250,000 cell numbers. Meshing on ANSYS ICEM-CFD is shown in Fig. 3 and Table 5.

Fig. 3. Meshing in ANSYS ICEM-CFD

Table 5
Parameters and values used in the simulation

Parameter	Value
Topology	Tetrahedron
Smoothing	High
Transition	Fast
Span Angle Center	Fine
Curvature Normal Angle	0.0024m
Minimum Size	0.0034m
Max Face Size	0.0045m
Growth Rate	Default
Minimum Edge Length	0.002m
Minimum Skewness	1.3×10^{-6}
Maximum Skewness	0.78974
Average Skewness	0.21859

2.9 Eulerian Multiphase Model

The Eurelian Multiphase model used in this study defines 3 phases, namely liquid, gas, and solid. Liquid is defined as the main phase in CFD arrangement while gas and solid as second phase. The inlet and outlet conditions of the primary phase are defined as velocity inlet and pressure outlet while the outlet condition of the second phase is defined as the pressure outlet. All walls are assumed under no slip. The volume of the gas phase fraction at the inlet and the liquid phase conditions at the outlet condition is set to 0. The volume of the solid phase fraction under inlet conditions is set to 2%. Liquid phase consists of a mixture of acetic acid, propionate, butyric and water. Liquid phase volume is patched as high as 15 cm from the base wall of the digester to the total digester height. The initial conditions of the mass fraction of acetic acid, propionate and butyrate are set to 0.0025 (2500 ppm), 0.0015 (1500 ppm), 0.002 (2000 ppm).

In this study, to simulate the gas-liquid-solid flow used Multiple Reference Frame (MRF) method as shown in Figure 2. MRF is generated around Rushton Impeller and shaft. When the MRF is activated, the motion equation will be modified by the addition of acceleration causing the change from the stationary wall into a moving wall. The rotation of the Rushton Impeller is set at 100 rpm in a well-regarded MRF arrangement for mixing in the digester. In this research, three-dimensional, three-dimensional Eulerian model is used to describe the flow behavior of each phase, so that liquid, biogas and sludge are treated as different continua. Therefore the three phases will have phase interactions with each other. In this study the interaction occurs in the liquid phase which will be degraded into solid phase and gas phase in the form of mud and biogas solids (methane, carbon dioxide, hydrogen). To simulate the biogas bubbles formed using seven bubble classes adjusted to the conditions of the digestion process which can be seen in Table 6 below [15].

Table 6
Bubble class and diameter

Bubble class (i)	Diameter (d_i) in (m)
1	0.0010
2	0.0015
3	0.0022
4	0.0032
5	0.0048
6	0.0071
7	0.0106

2.10 Material Properties

The material properties used in this simulation are shown in Table 7.

2.11 Solution and Discretization Methods

In this research, it is used the Phase Coupled SIMPLE (PC-SIMPLE) algorithm that combines pressure-velocity as the solution method. PC-SIMPLE is an enhanced SIMPLE algorithm for multiphase flow. This scheme uses split solving to find the solution of vector equations by each velocity of each phase being simulated. Then, the correction equation of pressure is built on the total continuity of the volume that is not the mass continuity. Pressure and speed are then

corrected to meet continuity issues. The discretization scheme used for each builder equation in the PC-SIMPLE solution method is "first order upwind" which includes momentum, fractional volume, kinetic energy, and turbulent dissipation ratio. For under relaxation factor can be seen in Table 8 below. The residual convergence criterion used is 10^{-3}. Time step used in this research is 0.01 s, while for initialization solution used hybrid initialization method.

Table 7
Material properties

Species	Density (kg m^{-1})	Heat Capacity (j kg^{-1})	Molecular weight (g mol^{-1})	Standard state enthalpy (kj $kmol^{-1}$)	Standard state enthalphy (kj $kmol^{-1}$ k^{-1})
Acetic acid	1,049	2,016	60.05	-483,880	158.00
Butyric acid	959.5	2,020	88.11	-533,900	226.30
Carbon dioxide	1.98	480	44.01	-393,532	213.72
Hydrogen	0.09	14,283	2.02	0	130.58
Methane	0.66	2,222	16.04	-74,895	186.04
Propionic acid	990	2,038	74.08	510,000	191.00
Water	998	4,182	18.01	-285,841	69.90
Sludge	1,250	-	-	-	-

Table 8
Under relaxation factor

Under relaxation factors	Value
Pressure	0.6
Density	1
Body force	1
Momentum	0.7
Volume fraction	0.6
Turbulent kinetic energy	0.6
Turbulent dissipation rate	0.6

3. Results and Discussion

3.1 Grid Independence Test

In a CFD simulation, the grid independence test is one of the important things. By doing a grid independence we can guarantee that the meshing we do is good and does not cause big errors in the simulation results. In this simulation, a grid independence test is conducted on five meshing methods with different cell numbers. The grid independence test is performed using a single phase flow with an initial velocity of 1 m/s by taking the velocity magnitude parameter in the integral report-volume section. This is done in order to save simulation time considering three phase simulation time which takes longer time. The error criterion is selected for < 1% to prove the grid independence. Table 9 shows the grid independence test results that have been done.

Furthermore, in this simulation used mesh with the number of cells as much as 250,000 with error of 0.75%. These results are considered meticulous enough to prove that the meshing/grid used does not cause large yield uncertainties.

Table 9
Grid independence test

Cell number	Velocity magnitude (m/s)	Error (%)
100,000	0.005907	0.87
150,000	0.00596	9.83
200,000	0.00661	1.93
250,000	0.00674	0.75

3.2 Validation Results

In this research, validation is done by comparing experimental data of propionate degradation to the result of simulation. Propionate degradation data taken from Amani et al experiments [11] as shown in Table 2. Experimental data were obtained after 30.5 hours of digging process, while simulation data was obtained for 175 seconds. Then through the experimental data obtained the equation of the line used to guess the concentration of propionate experimental results at the time obtained in the simulation. Table 10 shows the validation results between the experimental data and the simulation results in this study. After validation is done, then the next simulation variation of VFA concentration which will be compared to get the highest biogas production and methane gas concentration.

3.3 Mixer Effect on Digester

Figure 4 shows the contour of the liquid phase velocity distribution in the digester. The top speed is in the area around the impeller and the top of the digester. Performance of Rushton impeller with rotational speed of 100 rpm as a mixer in the digester is good enough, because the effect of rotation is uniform and can reach the entire digester part. This can be seen from the speed pathline profiles in Figures 4 and 5 showing the distribution of flow velocity on plane z = 41 mm. The plot XY curve of Fig. 6 shows a symmetrical speed distribution due to impeller rotation along the outer diameter of the digester, where the velocity will be minimal on the digester wall. Good mixing effectiveness will help accelerate the reaction that occurs within the digester and encourage the biogas that is formed to rise to the top of the digester.

Table 10
Concentration of Propionate

Time (second)	Concentration of Propionate				Error (%)
	Experimental Result		Experimental Result		
	(kmol/m^3)	(mg/L)	(kmol/m^3)	(mg/L)	
25	0.020333073	1506.274042	0.020212498	1497.341852	0.59%
50	0.020330023	1506.048118	0.020212498	1497.341852	0.58%
75	0.020326974	1505.822228	0.020212497	1497.341778	0.56%
100	0.020323925	1505.596371	0.020212493	1497.341481	0.55%
125	0.020320877	1505.370549	0.020212285	1497.326073	0.53%
150	0.020317829	1505.144760	0.020212469	1497.339704	0.52%
175	0.020314781	1504.919005	0.020212400	1497.334592	0.50%

The contours of the gas bubbles occurring in an anaerobic digging process in the digester are shown in Figure 7. The simulated results of the seven bubble classes show that the bubble with the largest diameter is at the top of the digester, while the smallest diameter bubble lies at the lower area of the digester around the impeller. This gas bubble size phenomenon is caused by the effects of turbulence, shear rate and buoyant force [15].

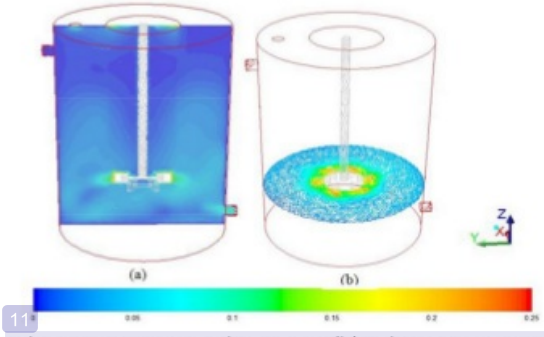

Fig. 4. (a) Liquid velocity contours on plane x = 0; (b) velocity vectors on plane z = 41 mm

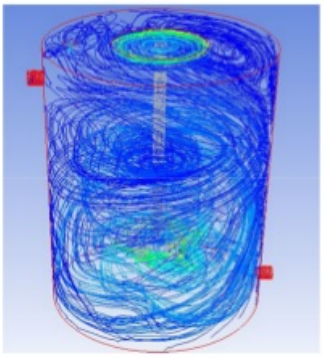

Fig. 5. Pathline of liquid velocity on plane x = 0

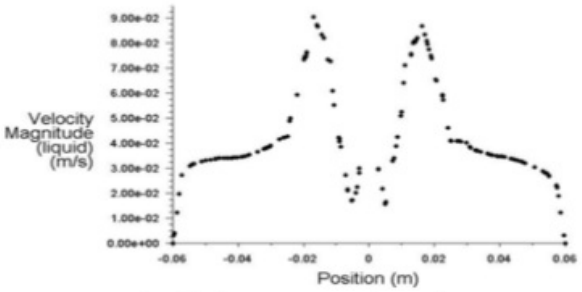

Fig. 6 Plot of velocity magnitude on plane z = 41 mm

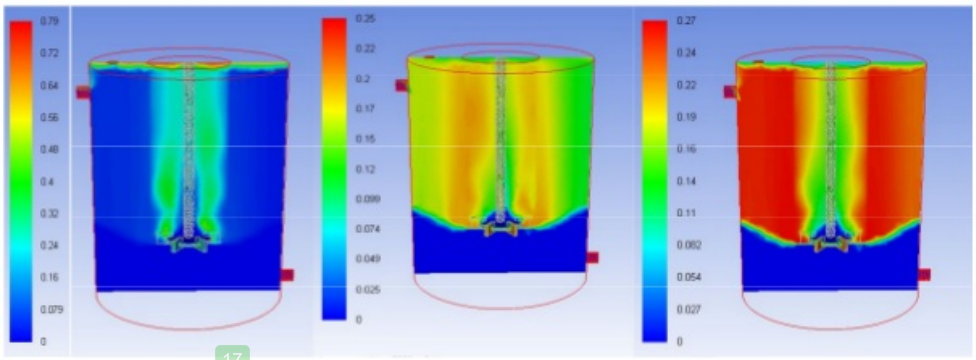

0.0106 m 0.0071 m 0.0048 m

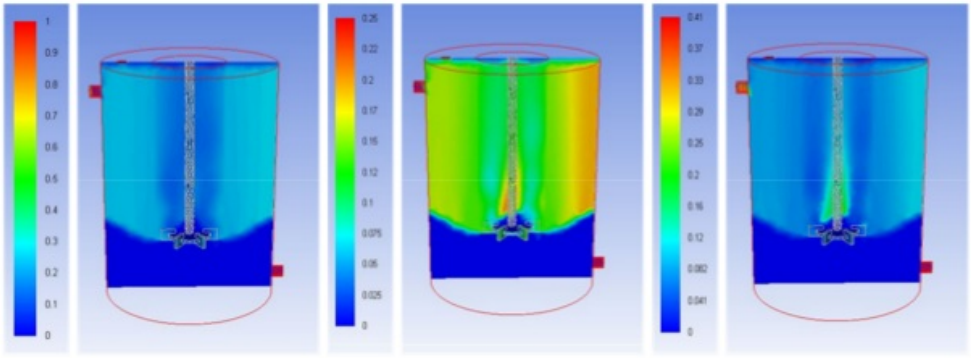

0.0032 m 0.0022 m 0.0015 m

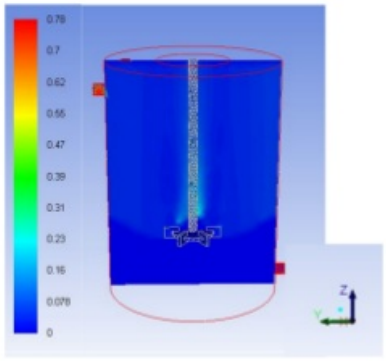

0.001 m

Fig. 7. Contour of class bubble distribution on plane x = 0

3.4 Analysis of Volatile Fatty Acid Concentrations (VFA) and Biogas

The ongoing chemical reactions between volatile fatty acids and water will encourage the formation of biogas (methane, hydrogen, and carbon dioxide). Because of these chemical reactions there will be a decrease in the concentration of VFA, as a chemical degradation phenomenon. The amount of concentration of biogas produced is influenced by the amount of input concentration of the VFA acting as the substrate, in addition to the mixing activity by the mixer which accelerates the reaction rate. In the validation model the concentration of VFA inputs consisted of propionic acid of 1.5 g/L, butyric acid of 2 g/L and acetic acid of 2.5 g/L.

The contour of molar concentration of volatile and biogas fatty acids at t = 70 s is shown in Figure 8 to 12. The concentration of each species of volatile fatty acid and biogas can be shown by selecting molar concentration species in the contour of the contour window, then in the select phase type what species phase is desired (liquid and gas). The biogas concentration is initially present at the bottom of the digester then due to the effect of the stirring being evenly distributed throughout the digester which will then be streamed out of the digester through the biogas outlet located on the top of the digester. The degradation of the substrate is obtained from the concentration value at the bottom outlet of the digester over time during the digestion process. As for biogas obtained from the value of concentrations contained in the outlet biogas.

For 70 seconds the VFA undergoes degdradasi organic matter converted into biogas. In actual circumstances, the process of synthetic interaction in the phase of acetogenesis and methanogenesis runs very long, so in the simulation of this final task the authors accelerate the reaction rate in order to obtain significant data by changing the pre exponential factor and activation energy (E) on FLUENT. The Pre Exponential Factor used in the simulation is 10^{15} and the activation energy is 108 J/kgmol. However, for initial validation it can be used the pre exponential factor and activation energy such as in literature. The pre exponential factor can be searched using the equation [16].

$$k = Ae^{-\frac{E}{RT}} \tag{11}$$

where:

k = constant rate of reaction ((kgmol/m^3)/day)
A = pre eksponential factor
E = activation energy(J/kgmol)
R = universal gas constant(J/kgmol-K)
T = temperature (K)

Table 11
Concentration variations in simulation

No	Parameter concentration	X (mg/L)	Y (mg/L)	Z (mg/L)
1	Variation-1	937	1,159	3,551
2	Variation-2	2,986	2,000	2,499
3	Variation-3	1,543	2,000	5,000
4	Variation-4	2,150	1,160	3,551
5	Variation-5	101	2,000	2,500
6	Variation-6	2,150	2,842	150
7	Variation-7	937	2,842	1,500

In this simulation, variation of substrate concentration was applied as many as seven variations with different composition. The initial concentration of propionate is denoted by the variable X, butyricates with Y and acetate are denoted by Z. This is done in order to avoid similarity, since the simulations performed have different pre exponential factor and activation energy values. Through this variation we will get the most optimum input concentration to produce biogas. Table 11 shows the substrate input concentration variation data conducted in this simulation.

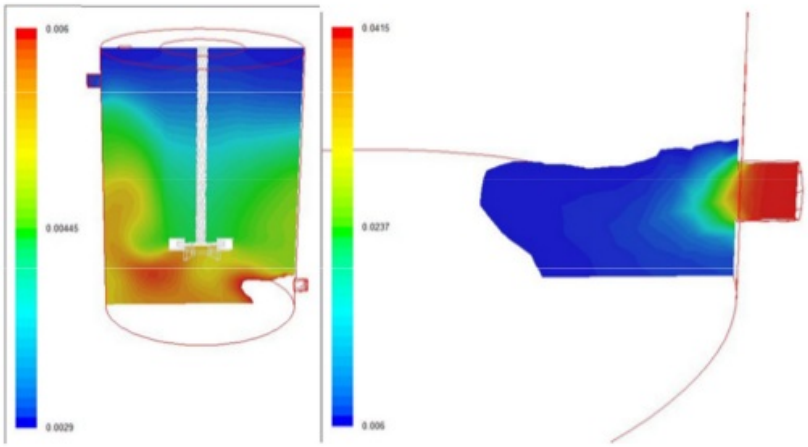

Fig. 8. Contour of molar concentration of acetate on plane x = 0

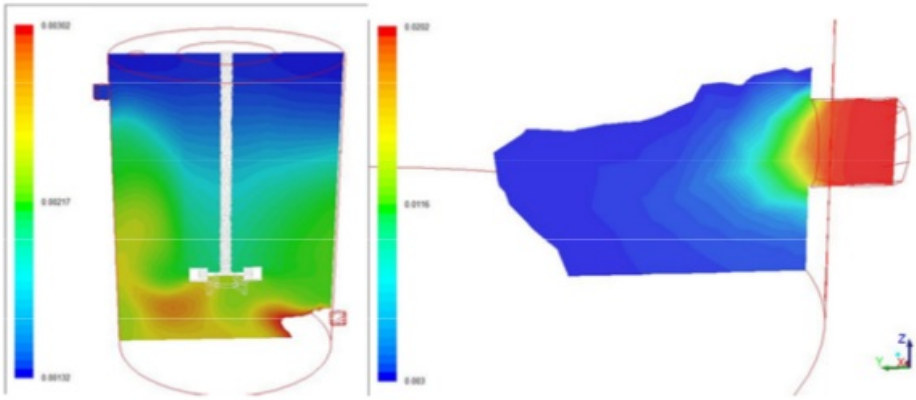

Fig. 9. Contour of molar concentration of propionate on plane x = 0

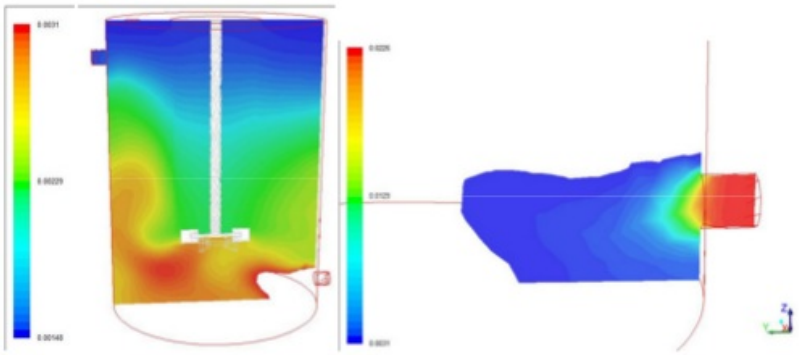

Fig. 10. Contours of molar concentration of butyrate on plane x = 0

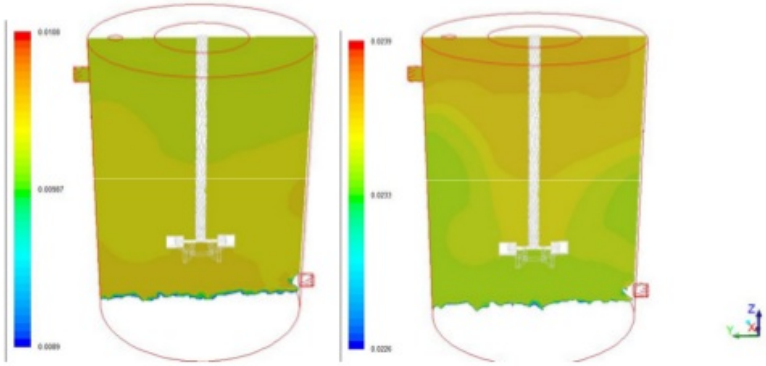

Fig. 11. Contours of molar concentration of CO_2 and H_2 on plane x = 0

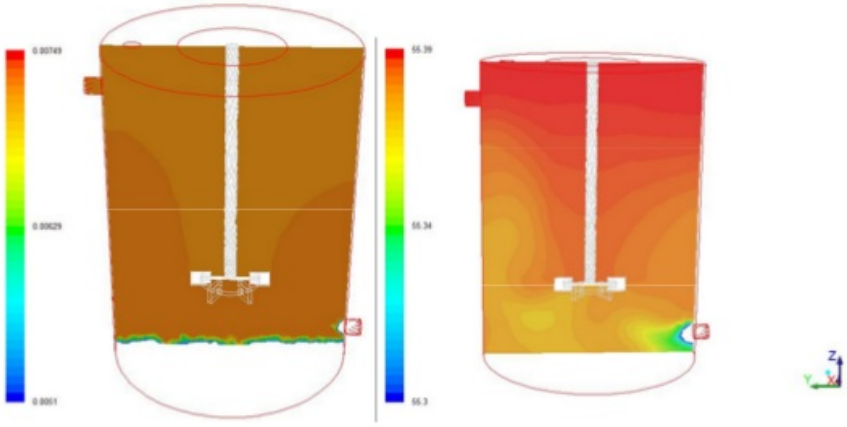

Fig. 12. Contours of molar concentrations of methane and water on plane x = 0

The concentration of the volatile fatty acid substrate will degrade over time, while the concentration of biogas will continue to increase with the commencement of biogas production, as shown in Figure 13. The speed of volatile fatty acid degradation differs from one variation to the other. This speed difference is due to the difference in input concentration compositions of volatile fatty acids that affect the rate of chemical reactions. Based on the data obtained, the highest biogas concentration was obtained in variation-3 with the biogas concentration of 0.9468 g/L, while the lowest was in the model with the biogas concentration of 0.6088 g/L.

The amount of methane concentration in the biogas produced varies between the digester models. The percentage of methane content was obtained by comparing the methane concentration with the biogas concentration obtained in the simulation. Figure 14 shows the methane concentration obtained from various digester variations for 70 s and Table 12 shows the percentage of average methane content contained in the simulated biogas during the 70 s digesting time. Table 12 shows that the largest methane content is generated on the variation-5 digester with the value of 22.96%, while the smallest is obtained at 17.62% in variation-6. Figure 14 also shows that the highest production of methane concentration is also produced in the variation-5 with value of 0.2328 g/L and the smallest variation in the reference model with value of 0.1128 g/L.

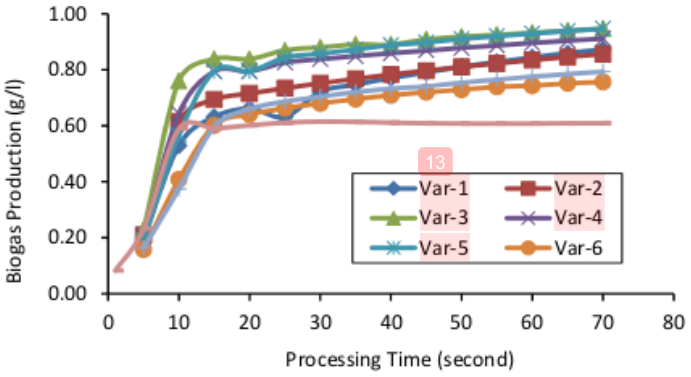

Fig. 13. Concentration of biogas production up to t = 70 seconds

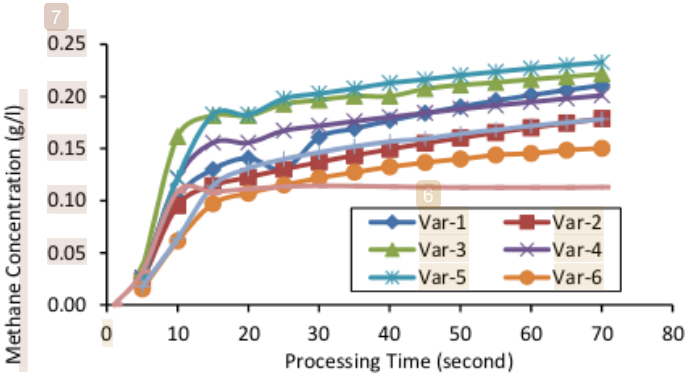

Fig. 14. Concentration of methane production to t = 70 seconds

Table 12
Methane content in biogas

Model Digester	The average content of methane in biogas (%)
Model	18.18%
Variation 1	21.77%
Variation 2	18.23%
Variation3	21.97%
Variation 4	20.23%
Variation 5	22.96%
Variation 6	17.62%
Variation 7	20.20%

4. Conclusion

The anaerobic digestion process in the digester can be modeled and simulated well using the Computational Fluid Dynamic method, through the equation of chemical reactions between species, which is indicated by the validation of the simulation results of the experiment, where the difference is quite small, less than 1%. Mixing causes a homogenization of the substrate of VFA with water, thereby speeding up the chemical reaction within the digester and encouraging the resulting biogas to rise to the top of the digester. Based on the simulation results of eight types of digester, the highest biogas content obtained in variation-3 with the value of 0.95 g/L, while the lowest production in the reference model with biogas content of 0.61 g/L. The largest concentration of methane is found in digesters with variation-5 with value of 0.2328 g/L (22.96%) and the smallest in the variation-6 with value of 17.62%.

Influence of Volatile Fatty Acid Concentration on Biogas Production in Synthropic Anaerobic Digestion

ORIGINALITY REPORT

10%	5%	8%	0%
SIMILARITY INDEX	INTERNET SOURCES	PUBLICATIONS	STUDENT PAPERS

PRIMARY SOURCES

1	H. Azargoshasb, S.M. Mousavi, T. Amani, A. Jafari, M. Nosrati. "Three-phase CFD simulation coupled with population balance equations of anaerobic syntrophic acidogenesis and methanogenesis reactions in a continuous stirred bioreactor", Journal of Industrial and Engineering Chemistry, 2015 Publication	4%
2	users.ugent.be Internet Source	1%
3	Azargoshasb, H., S.M. Mousavi, T. Amani, A. Jafari, and M. Nosrati. "Three-phase CFD simulation coupled with population balance equations of anaerobic syntrophic acidogenesis and methanogenesis reactions in a continuous stirred bioreactor", Journal of Industrial and Engineering Chemistry, 2015. Publication	1%
4	www.boem.gov Internet Source	<1%

5	nl.wikipedia.org Internet Source	<1%
6	repository.uinjkt.ac.id Internet Source	<1%
7	ir.lib.uwo.ca Internet Source	<1%
8	Galindo-García, Iván F., Ana K. Vázquez-Barragán, Alejandro G. Maní-González, and Miguel Rossano-Román. "CFD Simulation of Pollutant Emission in Power Plant Boilers", ASME 2011 Power Conference Volume 2, 2011. Publication	<1%
9	Majid Rasouli, Seyyed Mohammad Mousavi, Hamidreza Azargoshasb, Oveis Jamialahmadi, Yahya Ajabshirchi. "CFD simulation of fluid flow in a novel prototype radial mixed plug-flow reactor", Journal of Industrial and Engineering Chemistry, 2018 Publication	<1%
10	shopping.yahoo.com Internet Source	<1%
11	Kuo-Jen Hwang, Ya-Wen Hwang, Hideto Yoshida, Kazuha Shigemori. "Improvement of particle separation efficiency by installing conical top-plate in hydrocyclone", Powder Technology, 2012	<1%

Publication

12	Ricardo Gelves, A. Dietrich, Ralf Takors. "Modeling of gas–liquid mass transfer in a stirred tank bioreactor agitated by a Rushton turbine or a new pitched blade impeller", Bioprocess and Biosystems Engineering, 2013 Publication	<1%
13	www.marcopascali.com Internet Source	<1%
14	worldwidescience.org Internet Source	<1%
15	Rene Prieler, Martin Demuth, Davor Spoljaric, Christoph Hochenauer. "Evaluation of a steady flamelet approach for use in oxy-fuel combustion", Fuel, 2014 Publication	<1%
16	Yuzhen Jin, Jingyu Cui, Xiangdong Li, Hongli Chen. "An investigation on the distribution of massive fiber granules in rotor spinning units", Textile Research Journal, 2016 Publication	<1%
17	Sajjad Ahangar Zonouzi, Habibollah Safarzadeh, Habib Aminfar, Mousa Mohammadpourfard. "Experimental and numerical study of swirling subcooled flow boiling of water in a vertical annulus",	<1%

	Experimental Heat Transfer, 2018 Publication	
18	dias.library.tuc.gr Internet Source	<1%
19	www.australasianscience.com.au Internet Source	<1%
20	Zhang, Tian-Hu, Feng-Guo Liu, and Xue-Yi You. "Optimization of gas mixing system of premixed burner based on CFD analysis", Energy Conversion and Management, 2014. Publication	<1%
21	www.tandfonline.com Internet Source	<1%
22	scholarworks.uno.edu Internet Source	<1%
23	Jing, Dengwei, Li Jing, Huan Liu, Song Yao, and Liejin Guo. "Photocatalytic Hydrogen Production from Refinery Gas over a Fluidized-Bed Reactor I: Numerical Simulation", Industrial & Engineering Chemistry Research, 2013. Publication	<1%

Exclude quotes	Off	Exclude matches	Off
Exclude bibliography	Off		

Influence of Volatile Fatty Acid Concentration on Biogas Production in Synthropic Anaerobic Digestion

GRADEMARK REPORT

FINAL GRADE

/0

GENERAL COMMENTS

Instructor

PAGE 1

PAGE 2

PAGE 3

PAGE 4

PAGE 5

PAGE 6

PAGE 7

PAGE 8

PAGE 9

PAGE 10

PAGE 11

PAGE 12

PAGE 13

PAGE 14

PAGE 15

PAGE 16

PAGE 17

PAGE 18